

Differential Full Diversity Spatial Modulation using Amplitude Phase Shift Keying

Kavishaur DWARIKA¹, Hongjun XU^{1,2}

¹ School of Engineering, University of KwaZulu-Natal, King George V Avenue, 4041 Durban, South Africa

² School of Information and Electronic Engineering, Zhejiang Gongshang University, P.R. China

kavishaur@gmail.com, xuh@ukzn.ac.za

Submitted April 26, 2017 / Accepted November 10, 2017

Abstract. Diversity is a fundamental concept used to reduce the adverse effects of fading in wireless communications. Differential full diversity spatial modulation (DFD-SM) is a differential spatial modulation (DSM) scheme that makes use of a cyclic signaling phase shift keying (PSK) constellation to achieve transmit diversity. In this paper, firstly, we extend the work of DFD-SM to improve its throughput and/or error performance, by making use of an amplitude phase shift keying (APSK) constellation. Next, a power allocation concept (PAC) based on generalized differential modulation (GDM) is applied to DFD-SM using APSK. Finally we derive a theoretical upper bound on the average bit error probability (ABEP) for DFD-SM using APSK. It is shown through Monte Carlo simulations that the proposed DFD-SM using APSK scheme outperforms conventional DFD-SM by approximately 1 dB at the same throughput, and that the proposed power allocation scheme provides an approximate 3 dB gain over the conventional scheme.

Keywords

Spatial Modulation (SM), differential spatial modulation (DSM), full transmit diversity, amplitude phase shift keying (APSK)

1. Introduction

Spatial modulation (SM) [1] is a multiple-input multiple-output (MIMO) scheme that shows great promise for future wireless communication standards. In SM, information bits are partitioned into two parts. The first partition explicitly modulates the information bits to the symbols to be transmitted while the second partition implicitly conveys information bits based on the activation order of the transmit antennas. By having only a single transmit antenna active at any given instant in time, inter-channel interference (ICI) and inter-antenna synchronization (IAS) are entirely avoided [1]. SM however, requires full knowledge of the channel state information (CSI) at the receiver, which can be complicated to implement and adds to the system's overhead and complexity [2], [3].

As a result, differential spatial modulation (DSM) [2], [3] has been recently introduced. DSM eliminates the need for CSI, while maintaining the single transmit antenna property [3]. Consider an $N_R \times N_T$ DSM MIMO system [3], where N_R and N_T represent the total number of available receive and transmit antennas, respectively. DSM works for any constant value energy constellation, with M -ary phase shift keying (M -PSK) being the prevalent choice in literature [2–7]. DSM [3] has a spectral efficiency of $(\lfloor \log_2(N_T!) \rfloor + N_T \log_2(M)) / N_T$ bits/s/Hz, where $\lfloor \cdot \rfloor$ denotes the floor function. It is observed that the low complexity implementation at the receiver of DSM comes at a performance cost, as a 3 dB penalty is incurred, when compared to coherent SM [3]. DSM is capable of achieving receiver diversity of order N_R [4], which is the same as SM [1] and no transmit diversity. In order to improve error performance, multiple schemes that aim to achieve transmit diversity have been proposed [5–7] and will be briefly discussed.

In [5], a unified DSM (U-DSM) scheme which made use of a complex valued set of antenna index matrices was introduced. The number of redundant symbols transmitted by the DSM encoder is a design variable and could allow for transmit diversity gains at a reduced data rate. Thus a flexible rate-diversity tradeoff is achieved [5]. The system has a spectral efficiency of $(\lfloor \log_2(N_T!) \rfloor + N_T \log_2(M)/d) / N_T$ bits/s/Hz, where d , $1 \leq d \leq N_T$, is the transmit diversity order of the system. U-DSM is capable of achieving a diversity order of dN_R .

Differential full diversity spatial modulation (DFD-SM) in [6] proposed an $N_R \times 2$ DSM scheme which uses a set of L distinct cyclic unitary matrices to achieve full diversity. Two M -PSK ($L = M$) symbols are transmitted per block conveying $\log_2(L)$ information bits. The data rate is thus lower than that of [2], with a spectral efficiency of $(1 + \log_2(L)) / 2$ bits/s/Hz. DFD-SM ensures a diversity order of $2N_R$.

Field extension based DSM (FE-DSM) was proposed in [7] and develops a systematic design methodology to work for an arbitrary number of transmit antennas. FE-DSM transmits a single M -PSK symbol per space-time block and is thus able to achieve a diversity order of $N_R N_T$ at the cost of

DSM Scheme	No. of Transmit Antennas	Spectral Efficiency [bits/s/Hz]	Diversity Order
DSM [2]	2	$(1 + 2 \log_2(M)) / 2$	N_R
DSM [3]	N_T	$(\lfloor \log_2(N_T!) \rfloor + N_T \log_2(M)) / N_T$	N_R
U-DSM [5]	N_T	$(\lfloor \log_2(N_T!) \rfloor + N_T \log_2(M)/d) / N_T, 1 \leq d \leq N_T$	dN_R
DFD-SM [6]	2	$(1 + \log_2(M)) / 2$	$2N_R$
FE-DSM [7]	N_T	$\log_2(MN_T) / N_T$	$N_T N_R$
DSM using APSK method 1 [10]	N_T	$(\lfloor \log_2(N_T!) \rfloor + N_T \log_2(M) + 1) / N_T$	N_R
DSM using APSK method 2 [10]	N_T	$(\lfloor \log_2(N_T!) \rfloor + N_T \log_2(M) + N_T) / N_T$	N_R
High Rate DSM using APSK [11]	N_T	$(\lfloor \log_2(N_T!) \rfloor + N_T \log_2(M) + 2N_T) / N_T$	N_R

Tab. 1. Comparison between existing DSM schemes.

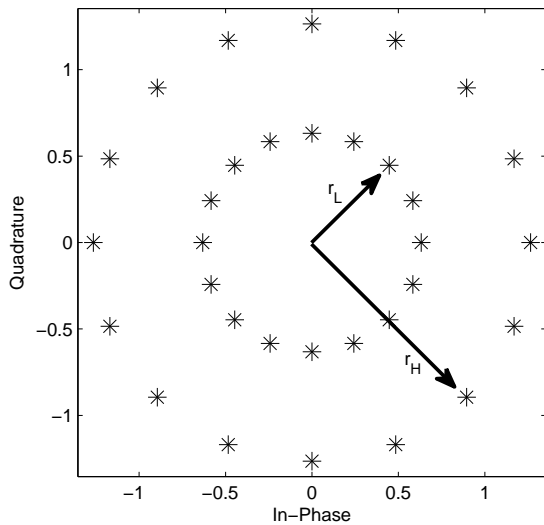


Fig. 1. 16 – 16 APSK constellation.

a reduced spectral efficiency of $\log_2(MN_T) / N_T$ bits/s/Hz. In favorable channel conditions, a rate-diversity trade-off scheme for FE-DSM was also introduced [7].

The schemes proposed in [2–7] utilize a unit M -PSK constellation so as to avoid power fluctuations during the differential encoding process. Differentially encoded amplitude phase shift keying (APSK) is an attractive alternative to differentially encoded M -PSK, as it has been seen to perform well in fading channels [8]. Xia in [9] proposed a differential scheme for Alamouti’s orthogonal space–time block code using APSK. The APSK constellation comprises of two independent M -PSK constellations and a single amplitude shift keying (ASK) constellation [9]. Figure 1 illustrates a 16 – 16 APSK constellation, where r_L and r_H denote the low and high amplitudes of the APSK constellation. $L - L$ APSK has a higher spectral efficiency when compared to M -PSK, since an additional information bit is used to toggle the amplitude of the symbols.

Martin in [10] implemented a DSM system that incorporates an $L - L$ APSK constellation. Two methods to differentially encode the amplitude of the transmitted symbols were introduced. The first method toggled the amplitude of all symbols being transmitted simultaneously by using a single information bit, resulting in a spectral efficiency of $(\lfloor \log_2(N_T!) \rfloor + N_T \log_2(M) + 1) / N_T$ bits/s/Hz.

The second method involved toggling each symbol’s amplitude independently, thus allowing for an additional N_T bits. The spectral efficiency of the second method is $(\lfloor \log_2(N_T!) \rfloor + N_T \log_2(M) + N_T) / N_T$ bits/s/Hz and thus achieves a higher throughput when compared to the first method, albeit, the computational complexity at the receiver is higher.

Extending the work of the second method from [10], a high-rate APSK DSM scheme was introduced in [11]. The APSK constellation comprises of four amplitude levels, thus allowing for a higher spectral efficiency of $(\lfloor \log_2(N_T!) \rfloor + N_T \log_2(M) + 2N_T) / N_T$ bits/s/Hz to be obtained. The system is seen to outperform [10] at the same throughput. A summary of all the presented DSM schemes can be found in Tab. 1.

When conventional differential modulation (CDM) is used, an approximate penalty of 3 dB is always incurred when compared to its coherent counterpart [12–14]. This is due to the nature of differential detection, which uses the noisy received signal from the preceding transmission to estimate the information contained in the current transmission, effectively doubling the noise power. In order to improve the error performance of CDM and reduce this 3 dB penalty, a generalized differential modulation (GDM) scheme was introduced in [12–14]. In GDM, a frame is split up into two parts, namely a reference part and a normal part. Both the reference and normal parts convey information. The reference block differentially encodes the normal blocks in the current frame and the reference block in the subsequent frame as opposed to CDM, which uses the previous block as a differential reference for the current block, as illustrated in Fig. 2. More power is allocated to the reference part as compared to the normal part, in order to improve the system’s error performance. It can be seen, that for a large enough frame length, the error performance of GDM can almost approach that of coherent detection [12–14].

Extending the work of GDM, a novel power allocation concept (PAC) was introduced in [15] for DFD-SM. The PAC uses a similar structure to GDM, however, only the normal blocks transmit information. A simplified framework was presented in order to find the optimal power distribution among the normal and reference blocks to achieve the

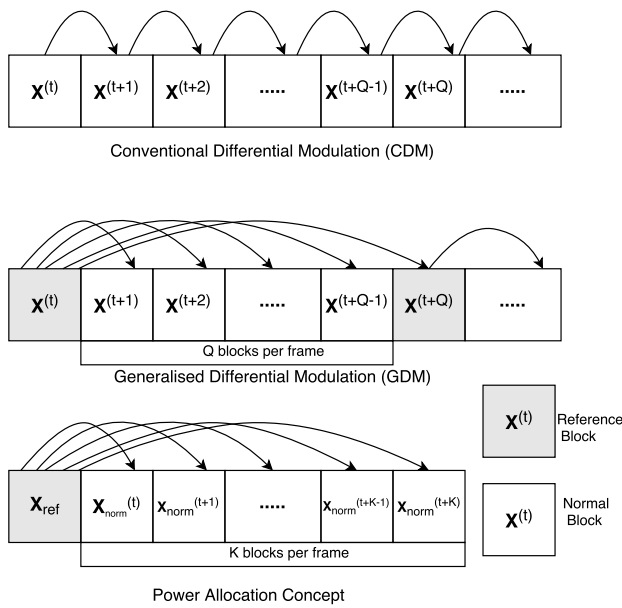


Fig. 2. Comparison between CDM, GDM and the PAC.

best error performance. The PAC can be applied to any differential modulation scheme [15], provided a unit M -PSK constellation is used. Figure 2 illustrates the differential encoding procedures of CDM, GDM and the PAC. It can be observed that the PAC transmits each frame independently of the preceding frame, when compared to CDM and GDM.

Although the DSM schemes that incorporate transmit diversity techniques [5–7] or an APSK constellation [10], [11] display superior error performance over conventional DSM [2], [3], their true error performance potential is not realized, since they will always incur a penalty of approximately 3 dB when compared to their coherent equivalents. From Tab. 1, it can be observed that no DSM scheme using APSK (non M -PSK) is yet to achieve full diversity. The work of [9–11] motivates us to utilize an APSK constellation with DFD-SM [6] to further improve its spectral efficiency and error performance, which will be referred to as DFD-SM using APSK, while maintaining a diversity order of $2N_R$. Next, we extend the power allocation concept (PAC) from [15] and apply it to DFD-SM using APSK in order to reduce the 3 dB penalty that differential detection is susceptible to. A framework is presented to incorporate an APSK constellation with the PAC.

The rest of the paper is organized as follows: Section 2 is broken down into 3 subsections. Section 2.1 gives a brief overview of conventional DFD-SM and introduces its system model. Section 2.2 introduces the proposed DFD-SM using APSK scheme and Section 2.3 discusses the implementation of the PAC [15] to the proposed system. In Sec. 3, a derivation of the asymptotic upper bound on the average bit error probability (ABEP) of the proposed system is provided. Section 4 provides the simulation results and discussion and finally Sec. 5 concludes the paper.

Notation used in this paper: Bold upper/lower case letters represent matrices/vectors. $(\cdot)^T$, $(\cdot)^H$, and $(\cdot)^*$ represent the transpose, Hermitian and complex conjugate operations, respectively. $\text{Tr}(\mathbf{X})$ denotes the trace operation and $\|\cdot\|_F^2$ denotes the Frobenius norm. $\arg \max$ and $\arg \min$ returns the maximum and minimum argument passed to it, respectively and $(\cdot)!!$ denotes the double factorial operator. $Q(x) = \frac{1}{\sqrt{2\pi}} \int_x^\infty \exp\left(-\frac{t^2}{2}\right) dt$ denotes the Gaussian error function and $E_{\mathbf{H}}[\cdot]$ denotes the expectation over the fading channel \mathbf{H} .

2. System Model

In this section, the system model of conventional DFD-SM (CDFD-SM), comprising of two transmit antennas and N_R receive antennas, is first introduced. We next introduce the system model for DFD-SM using APSK. Based on the PAC of [15], we finally discuss the system model of the PAC applied to DFD-SM using APSK. Each system is assumed to have two transmit antennas, $N_T = 2$, and N_R receive antennas.

2.1 Conventional DFD-SM (CDFD-SM)

In CDFD-SM, the information bit stream is partitioned into two parts and mapped to indices (q, l) . Index $q \in \{0, 1\}$ consists of one $(\log_2(N_T))$ information bit and determines the selected antenna activation order matrix \mathbf{A}_q , where [6]

$$\mathbf{A}_0 = \begin{bmatrix} 1 & 0 \\ 0 & 1 \end{bmatrix}, \mathbf{A}_1 = \begin{bmatrix} 0 & \exp(j\phi) \\ \exp(j\phi) & 0 \end{bmatrix}. \quad (1)$$

Index $l \in \{0, 1, \dots, L-1\}$ consists of $\log_2(L)$ information bits and determines the selected codeword $\mathbf{V}_l = \text{diag}\left(\exp\left(\frac{j2\pi u_1 l}{L}\right), \exp\left(\frac{j2\pi u_2 l}{L}\right)\right)$, where \mathbf{V}_l is drawn from a cyclic signaling unitary constellation [6]. The optimization of parameters u_1, u_2 and ϕ are discussed in [6], in order to attain a full diversity order. Thus, it can be seen that a total of $1 + \log_2(L)$ information bits are transmitted per block.

In the t^{th} block of transmission, a $\mathbb{C}^{2 \times 2}$ signal matrix which encodes the space and time dimensions is defined as $\mathbf{S}^{(t)} = \mathbf{A}_q^{(t)} \mathbf{V}_l^{(t)}$. The signal matrix is then differentially encoded into a $\mathbb{C}^{2 \times 2}$ space-time matrix as $\mathbf{X}^{(t)} = \mathbf{X}^{(t-1)} \mathbf{S}^{(t)}$. In the initial block, the differentially encoded space-time matrix is set as $\mathbf{X}^{(0)} = \mathbf{I}_2 = \mathbf{V}_0$, where \mathbf{I}_2 represents the 2×2 identity matrix, for simplicity.

The received signal in the t^{th} block is given by

$$\mathbf{Y}^{(t)} = \mathbf{H}^{(t)} \mathbf{X}^{(t)} + \mathbf{N}^{(t)} \quad (2)$$

where $\mathbf{H}^{(t)} \in \mathbb{C}^{N_R \times 2}$ and $\mathbf{N}^{(t)} \in \mathbb{C}^{N_R \times 2}$ are the fading channel matrix and additive white Gaussian noise (AWGN) channel matrix of the t^{th} transmission, respectively, whose entries are complex-valued, independent and identically distributed (i.i.d) Gaussian random variables (RVs) with $\mathcal{CN}(0, 1)$ and $\mathcal{CN}(0, \sigma_n^2)$ distributions, respectively. It can be seen that

the system has an average signal-to-noise ratio (SNR) of $\bar{\gamma}_n = \frac{1}{\sigma_n^2}$. Assuming quasi-static fading, $\mathbf{H}^{(t)} = \mathbf{H}^{(t-1)}$, the maximum-likelihood (ML) detector can be derived as [6]

$$(\hat{q}, \hat{l}) = \arg \max_{\substack{\hat{q} \in \{0:1\} \\ \hat{l} \in \{0:L-1\}}} \Re \left[\text{Tr} \left(\left(\mathbf{Y}^{(t)} \right)^H \mathbf{Y}^{(t-1)} \mathbf{A}_{\hat{q}} \mathbf{V}_{\hat{l}} \right) \right]. \quad (3)$$

2.2 DFD-SM using APSK

This section introduces the system model for DFD-SM using APSK, as illustrated in Fig. 3. In CDFD-SM, we observe that one block requires two M -PSK symbols to be transmitted, in order to convey $\log_2(M)$ information bits. Based on this, we opt to encode the amplitude of the entire transmit block and thus use the first method from [10]. Although the second method [10] has a higher spectral efficiency, an increase in computational complexity will be required at the receiver. The system can be extended to any number of amplitude levels, but for the purposes of this paper, we will consider the first method.

Let r_L and r_H denote the low and high radii of the $L - L$ APSK constellation, respectively. The radii are set as $r_H = 1.265$ and $r_L = 0.632$ to satisfy the ring ratio criterion of $\frac{r_H}{r_L} = 2$ and $(r_H^2 + r_L^2)/2 = 1$ [9]. Since an ASK constellation is being added to the cyclic signaling M -PSK constellation, the design of parameters (u_1, u_2, ϕ) will remain the same as in [6].

In the t^{th} block, $\log_2(L) + 2$ information bits are mapped to (b, q, l) where $b \in \{0, 1\}$ toggles the amplitude of the transmitted symbols according to [9], [10] as

$$r_c^{(t)} = \begin{cases} 1, & \text{if } b = 0, \\ \frac{r_H}{r_L}, & \text{if } b = 1 \text{ and } a^{(t-1)} = r_L, \\ \frac{r_L}{r_H}, & \text{if } b = 1 \text{ and } a^{(t-1)} = r_H \end{cases} \quad (4)$$

where $a^{(t-1)} \in \{r_L, r_H\}$ is the amplitude of the previous transmission $\mathbf{X}^{(t-1)}$. The signal matrix is now differentially encoded in a $\mathbb{C}^{2 \times 2}$ space-time matrix as $\mathbf{X}^{(t)} = r_c^{(t)} \mathbf{X}^{(t-1)} \mathbf{S}^{(t)}$. In the initial transmission, the differentially encoded matrix is set as $\mathbf{X}^{(0)} = r_L \mathbf{I}_2$, where $a^{(0)} = r_L$.

Based on the received signal in (2), the received signal for DFD-SM using APSK can be re-written as

$$\mathbf{Y}^{(t)} = r_c^{(t)} \mathbf{Y}^{(t-1)} \mathbf{A}_q^{(t)} \mathbf{V}_l^{(t)} - r_c^{(t)} \mathbf{N}^{(t-1)} \mathbf{A}_q^{(t)} \mathbf{V}_l^{(t)} + \mathbf{N}^{(t)}. \quad (5)$$

From (5), the ML detector can be derived as

$$(\hat{b}, \hat{q}, \hat{l}) = \arg \min_{\substack{\hat{b} \in \{0:1\} \\ \hat{q} \in \{0:1\} \\ \hat{l} \in \{0:L-1\}}} \left\| \mathbf{Y}^{(t)} - \hat{r}_c^{(t)} \mathbf{Y}^{(t-1)} \mathbf{A}_{\hat{q}} \mathbf{V}_{\hat{l}} \right\|_F^2 \quad (6)$$

where $\hat{r}_c^{(t)} \in \left\{ 1, \frac{r_L}{r_H}, \frac{r_H}{r_L} \right\}$.

2.3 PAC for DFD-SM using APSK

In this subsection, we apply the PAC introduced in [15] to DFD-SM using APSK. The PAC exploits the fact that

the differential detector is considered to have an *estimation-detection* structure [12]. This implies that the previous received block, is used as an estimation to the fading channel matrix, in order to coherently detect the information conveyed in the current received block [12].

Each frame is assumed to contain $(K + 1)$ blocks. K blocks, defined as normal blocks, will convey information. The first block transmitted in a frame, defined as a reference block, will serve as reference to the subsequent K normal blocks in the frame [15].

The reference (first) block transmitted in a frame is given by [15]

$$\mathbf{Y}_{\text{ref}} = \mathbf{H}_{\text{ref}} \mathbf{X}_{\text{ref}} + \mathbf{N}_{\text{ref}} \quad (7)$$

where $\mathbf{X}_{\text{ref}} = \mathbf{I}_2 = \mathbf{V}_0$. The entries of \mathbf{N}_{ref} are i.i.d. complex Gaussian RVs with a $\mathcal{CN}(0, \sigma_{\text{ref}}^2)$ distribution. Thus, the reference block has an average SNR of $\bar{\gamma}_{\text{ref}} = \frac{1}{\sigma_{\text{ref}}^2} = (1 + K\alpha)\bar{\gamma}$, where α is the fraction of power extracted from the K normal blocks and is allocated to the reference block [15]. The remaining K received normal blocks are given by

$$\mathbf{Y}_{\text{norm}}^{(t)} = \mathbf{H}_{\text{norm}}^{(t)} \mathbf{X}_{\text{norm}}^{(t)} + \mathbf{N}_{\text{norm}}^{(t)}, \quad 1 \leq t \leq K \quad (8)$$

where $\mathbf{X}_{\text{norm}}^{(t)} = r_p^{(t)} \mathbf{X}_{\text{ref}} \mathbf{S}^{(t)}$. Since the proposed scheme does not rely on any knowledge of the previous transmission $\mathbf{X}_{\text{norm}}^{(t-1)}$ and only relies on $\mathbf{X}_{\text{ref}} = \mathbf{V}_0$, the definition of $r_c^{(t)}$ changes to

$$r_p^{(t)} = \begin{cases} r_L, & \text{if } b = 0, \\ r_H, & \text{if } b = 1. \end{cases} \quad (9)$$

Note that the radius of the signal matrix is directly set by the selected bit, as opposed to changing the radius as seen in (4). The entries of $\mathbf{N}_{\text{norm}}^{(t)}$ are also i.i.d. complex Gaussian RVs with a $\mathcal{CN}(0, \sigma_{\text{norm}}^2)$ distribution. Thus, the normal block has an average SNR of $\bar{\gamma}_{\text{norm}} = \frac{1}{\sigma_{\text{norm}}^2} = (1 - \alpha)\bar{\gamma}$ [15].

Assuming that $\mathbf{H}_{\text{ref}} = \mathbf{H}_{\text{norm}}^{(t)}$, $1 \leq t \leq K$, we can re-write the received signal in (8) as

$$\mathbf{Y}_{\text{norm}}^{(t)} = r_p^{(t)} \mathbf{Y}_{\text{ref}} \mathbf{A}_q^{(t)} \mathbf{V}_l^{(t)} - r_p^{(t)} \mathbf{N}_{\text{ref}} \mathbf{A}_q^{(t)} \mathbf{V}_l^{(t)} + \mathbf{N}_{\text{norm}}^{(t)}. \quad (10)$$

If we analyze the received signal in (10), it is obvious that the signal contains two noise elements comprising of two different variances. The effective or total noise variance of (10) can be calculated as

$$\sigma_{\text{eff}}^2 = \sigma_{\text{ref}}^2 + \sigma_{\text{norm}}^2. \quad (11)$$

The ML detector can now be derived following (10) as

$$(\hat{b}, \hat{q}, \hat{l}) = \arg \min_{\substack{\hat{b} \in \{0:1\} \\ \hat{q} \in \{0:1\} \\ \hat{l} \in \{0:L-1\}}} \left\| \mathbf{Y}_{\text{norm}}^{(t)} - \hat{r}_p^{(t)} \mathbf{Y}_{\text{ref}} \mathbf{A}_{\hat{q}} \mathbf{V}_{\hat{l}} \right\|_F^2 \quad (12)$$

where $\hat{r}_p^{(t)} \in \{r_L, r_H\}$.

In [15], the optimum value of α is derived by minimizing the effective noise variance, which was found to be

$$\alpha_{\text{opt}} = \frac{\sqrt{K} - 1}{\sqrt{K} + K}. \quad (13)$$

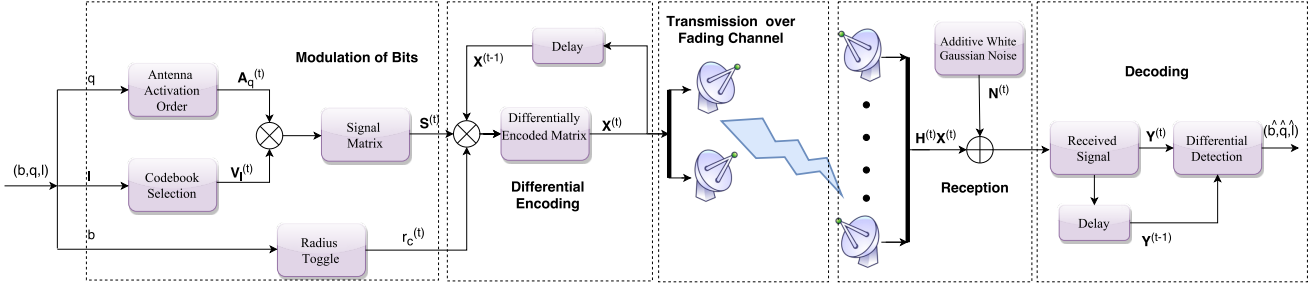


Fig. 3. System model of DFD-SM using APSK.

When selecting the value of K , one should be mindful of the peak to average power ratio (PAPR) required [12], as well as the block duration for which the channel remains constant [15], since [10] reports severe performance degradation in fast fading channels.

3. Asymptotic Error Performance Analysis

We follow the method used in [11] to derive the asymptotic upper bound on the average bit error probability (ABEP) for DFD-SM using APSK. Using the union bound method, the ABEP for DFD-SM using APSK is given by

$$\text{ABEP} \leq \frac{1}{N_b 2^{N_b}} \sum_{\mathbf{X}^{(t)}} \sum_{\substack{\hat{\mathbf{X}}^{(t)} \\ \hat{\mathbf{X}}^{(t)} \neq \mathbf{X}^{(t)}}} N(\mathbf{X}^{(t)}, \hat{\mathbf{X}}^{(t)}) P(\mathbf{X}^{(t)} \rightarrow \hat{\mathbf{X}}^{(t)}) \quad (14)$$

where $N_b = 2 + \log_2(L)$ is the total number of bits conveyed by a single transmit block, $\mathbf{X}^{(t)}$ is the set of all legitimate transmit symbols, $P(\mathbf{X}^{(t)} \rightarrow \hat{\mathbf{X}}^{(t)})$ is the pairwise error probability (PEP) given that $\mathbf{X}^{(t)}$ was transmitted and $\hat{\mathbf{X}}^{(t)}$ was decoded and $N(\mathbf{X}^{(t)}, \hat{\mathbf{X}}^{(t)})$ is the number of bits in difference between $\mathbf{X}^{(t)}$ and $\hat{\mathbf{X}}^{(t)}$. With the assumption that $\hat{\mathbf{X}}^{(t-1)}$ is right [11], following (6) we have

$$P(\mathbf{X}^{(t)} \rightarrow \hat{\mathbf{X}}^{(t)}) = P\left(\left\|\mathbf{Y}^{(t)} - r_c^{(t)} \mathbf{Y}^{(t-1)} \mathbf{S}^{(t)}\right\|_F^2 - \left\|\mathbf{Y}^{(t)} - \hat{r}_c^{(t)} \mathbf{Y}^{(t-1)} \hat{\mathbf{S}}^{(t)}\right\|_F^2 > 0\right). \quad (15)$$

Substituting $\mathbf{Y}^{(t)} = \mathbf{H}\mathbf{X}^{(t)} + \mathbf{N}^{(t)}$ and $\mathbf{Y}^{(t-1)} = \mathbf{H}\mathbf{X}^{(t-1)} + \mathbf{N}^{(t-1)}$, where $\mathbf{H}^{(t)} = \mathbf{H}^{(t-1)} = \mathbf{H}$, we can simplify (15) into

$$P(\mathbf{X}^{(t)} \rightarrow \hat{\mathbf{X}}^{(t)}) = P\left(\left\|\mathbf{W}_1\right\|_F^2 > \left\|\mathbf{H}(\mathbf{X}^{(t)} - \hat{\mathbf{X}}^{(t)}) + \mathbf{W}_2\right\|_F^2\right) \quad (16)$$

where $\mathbf{W}_1 = \mathbf{N}^{(t)} - r_c^{(t)} \mathbf{N}^{(t-1)} \mathbf{S}^{(t)}$ and $\mathbf{W}_2 = \mathbf{N}^{(t)} - \hat{r}_c^{(t)} \mathbf{N}^{(t-1)} \hat{\mathbf{S}}^{(t)}$. Let $\mathbf{D} = \mathbf{H}(\mathbf{X}^{(t)} - \hat{\mathbf{X}}^{(t)}) = [\mathbf{d}_1, \mathbf{d}_2]$, where $\mathbf{d}_i \in \mathbb{C}^{N_R \times 1}$, $i \in \{1, 2\}$ denotes the column vectors of \mathbf{D} , (16) can be represented as

$$P(\mathbf{X}^{(t)} \rightarrow \hat{\mathbf{X}}^{(t)}) = P(\zeta > \|\mathbf{D}\|_F^2) \quad (17)$$

where $\zeta = \text{Tr}(\mathbf{W}_2^H \mathbf{D} + \mathbf{D}^H \mathbf{W}_2)$ [11]. For any given channel realization, it can be seen that ζ is a complex-valued Gaussian RV with zero mean and variance of $\sigma_\zeta^2 = 2\sigma_n^2(1 + |\hat{r}_c^{(t)}|^2) \|\mathbf{D}\|_F^2$ [11]. For all possible $\mathbf{X}^{(t-1)}$, the average value of $|\hat{r}_c^{(t)}|^2$ is 1 [11], and thus follows a $\mathcal{CN}(0, 4\sigma_n^2 \|\mathbf{D}\|_F^2)$ distribution. Hence the PEP can be determined as

$$P(\mathbf{X}^{(t)} \rightarrow \hat{\mathbf{X}}^{(t)}) = E_{\mathbf{H}} \left[Q \left(\sqrt{\frac{\|\mathbf{H}(\mathbf{X}^{(t)} - \hat{\mathbf{X}}^{(t)})\|_F^2}{4\sigma_n^2}} \right) \right]. \quad (18)$$

Let $\mathbf{\Delta} = (\mathbf{X}^{(t)} - \hat{\mathbf{X}}^{(t)}) = [\mathbf{\Upsilon}_1, \mathbf{\Upsilon}_2]^T$ and $\mathbf{H} = [\mathbf{h}_1, \mathbf{h}_2]$, where $\mathbf{\Upsilon}_i \in \mathbb{C}^{1 \times 2}$ and $\mathbf{h}_i \in \mathbb{C}^{N_R \times 1}$ denotes the i^{th} row of $\mathbf{\Delta}$ and the i^{th} row of \mathbf{H} , respectively, $i \in \{1, 2\}$, we can simplify the numerator of (18) as [11]

$$E_{\mathbf{H}} [\|\mathbf{H}\mathbf{\Delta}\|_F^2] = E_{\mathbf{H}} \left[\sum_{i=1}^{\kappa} \|\mathbf{\Upsilon}_{v_i}\|_F^2 \|\mathbf{h}_{v_i}\|_F^2 \right] \quad (19)$$

where κ is the number of non-zero elements in $\{\mathbf{\Upsilon}_i\}_{i=1}^2$ and $\{v_i\}_{i=1}^{\kappa}$ are the corresponding indices of the non-zero elements [11]. Due to the nature of the cyclic signalling set being used, the rank of $\mathbf{\Delta}$ is 2, provided $\mathbf{\Delta} \neq 0$ and thus full diversity of order $2N_R$ is obtained [6]. According to [11], it can be seen that the variable $2\|\mathbf{h}_i\|_F^2$ follows a Chi-squared distribution with $2N_R$ degrees of freedom, whose probability density function (PDF) is given by [11]

$$f_{2\|\mathbf{h}_i\|_F^2}(x) = \left(\frac{1}{2}\right)^{N_R} \frac{x^{(N_R-1)} \exp(-x/2)}{(N_R-1)!}, \quad x \geq 0. \quad (20)$$

Using Craig's alternate form of the Gaussian error function, $Q(x) = \frac{1}{\pi} \int_0^{\pi/2} \exp\left(\frac{-x^2}{2\sin^2(\theta)}\right) d\theta$ and (20), (18) can be represented as

$$P(\mathbf{X}^{(t)} \rightarrow \hat{\mathbf{X}}^{(t)}) = \frac{1}{\pi} \int_0^{\pi/2} \prod_{i=1}^{\kappa} \left(\int_0^{\infty} \frac{x^{(N_R-1)}}{(N_R-1)!} \exp\left[-\left(1 + \frac{\|\mathbf{\Upsilon}_{v_i}\|_F^2}{8\sigma_n^2 \sin^2(\theta)}\right)x\right] dx \right) d\theta \leq \frac{1}{\pi} \int_0^{\pi/2} \prod_{i=1}^{\kappa} \left(\frac{8\sigma_n^2 \sin^2(\theta)}{\|\mathbf{\Upsilon}_{v_i}\|_F^2} \right)^{N_R} d\theta. \quad (21)$$

Using the double factorial identity $\int_0^{\pi/2} \sin^n(x) dx = \frac{(n-1)!!}{n!!} \left(\frac{\pi}{2}\right)$ for n being any even integer, we have (21) in a closed form as

$$P(\mathbf{X}^{(t)} \rightarrow \hat{\mathbf{X}}^{(t)}) \leq \frac{\sigma_n^{(2\kappa N_R)} 8^{(\kappa N_R)} (2\kappa N_R - 1)!!}{2 \left(\|\mathbf{Y}_{v_i}\|_F^2 \cdots \|\mathbf{Y}_{v_k}\|_F^2 \right)^{N_R} (2\kappa N_R)!!} \quad (22)$$

Substituting (22) into (14), a closed form of the upper bound on the ABEP can be obtained. The upper bound of the ABEP for the PAC applied to DFD-SM using APSK, can be found in the appendix.

4. Simulations

For the simulations, a quasi-static Rayleigh fading channel was assumed. The simulations were performed for one and two receive antennas. For fairness of comparison, all systems have a spectral efficiency of 3 bits/s/Hz. First, we compare DFD-SM using a 16 – 16 APSK constellation with parameters $(L, u_1, u_2, \phi) = (16, 1, 7, \pi/4)$ against CDFD-SM [6] using a 32-PSK constellation with parameters $(L, u_1, u_2, \phi) = (32, 1, 15, \pi/4)$. The PAC applied to DFD-SM using APSK and DFD-SM using APSK with coherent transmission/detection are included in Fig. 4 and 5, which have the same parameters as DFD-SM using a 16 – 16 APSK constellation. DSM [1], [2] with two transmit antennas, which transmits a symbol drawn from an 8-PSK constellation in the first time slot and a symbol drawn from a 4-PSK constellation in the second time slot (in order to maintain a spectral efficiency of 3 bits/s/Hz), is included for reference.

It can be seen that DFD-SM using APSK outperforms CDFD-SM. If we consider a BER of 10^{-4} , we observe that DFD-SM using APSK has an approximate 1 dB gain over CDFD-SM, while the power allocation scheme outperforms CDFD-SM by approximately 3 dB and DFD-SM using APSK by approximately 2 dB. It can be seen that the power allocation scheme is approximately 1 dB behind that of DFD-SM using APSK with coherent transmission/detection.

Next, we investigate the effect the frame length has on the error performance. We choose a frame length of $K = 100$ and $K = 400$ for comparison in Fig. 6. We observe a marginal gain of about 0.5 dB at a target BER of 10^{-5} for an increase in frame length. Thus, as $K \rightarrow \infty$, coherent performance can almost be achieved.

According to [6], [11], the upper bound placed on the exponential function as seen in (21) results in the ABEP being an approximation of the performance in the high SNR region. From Sec. 2.3, it is obvious that $\sigma_{\text{norm}}^2 \gg \sigma_{\text{ref}}^2$. Thus we can assume that $\sigma_{\text{eff}}^2 \approx \sigma_{\text{norm}}^2$ at high SNR. Substituting this approximation into (28), an improved approximation of the ABEP can be obtained, as seen in Fig. 7. The new bound is seen to be much tighter in the high SNR region, when compared to the original bound.

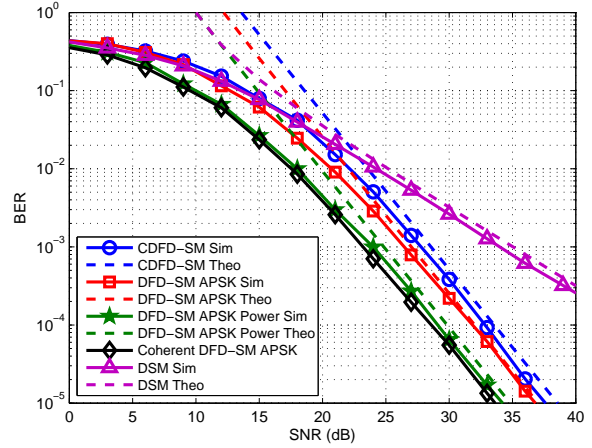


Fig. 4. BER of CDFD-SM, DFD-SM using APSK and the PAC applied to DFD-SM using APSK $N_R = 1$.

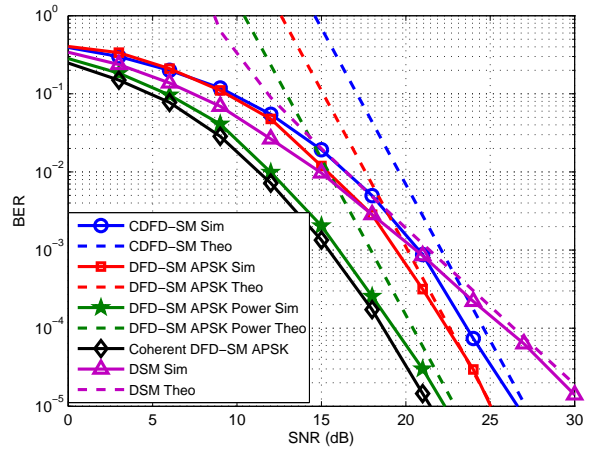


Fig. 5. BER of CDFD-SM, DFD-SM using APSK and the PAC applied to DFD-SM using APSK $N_R = 2$.

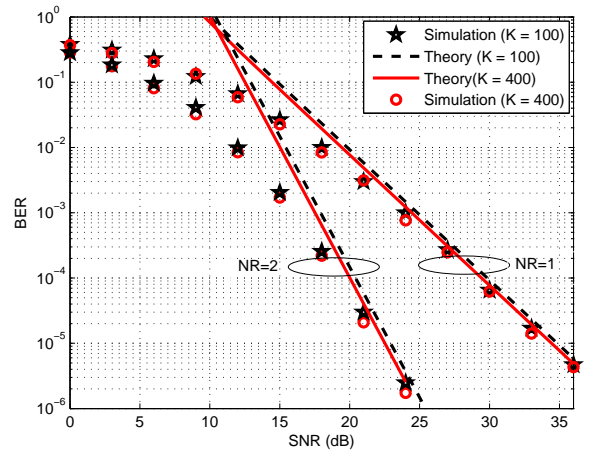


Fig. 6. PAC applied to DFD-SM using APSK for $K = 100$ and $K = 400$.

Finally, we verify that α_{opt} [15] minimizes the bit error performance for DFD-SM using APSK. Using (13), we have $\alpha_{\text{opt}} = 0.0818$ for $K = 100$. Figure 8 contains a plot of the ABEP (28) as a function of α , at $\bar{\gamma} = 36$ dB for $N_R = 1$ and $\bar{\gamma} = 20$ dB for $N_R = 2$, respectively. From Fig. 8, we observe that the BER is a minimum when $\alpha = \alpha_{\text{opt}}$.

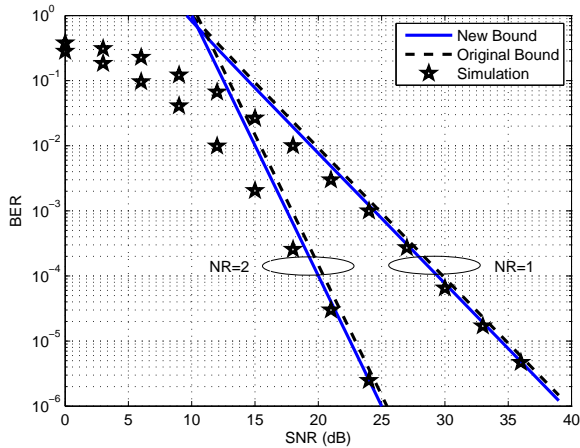


Fig. 7. High SNR Bound of the PAC applied to DFD-SM using APSK with $K = 100$.

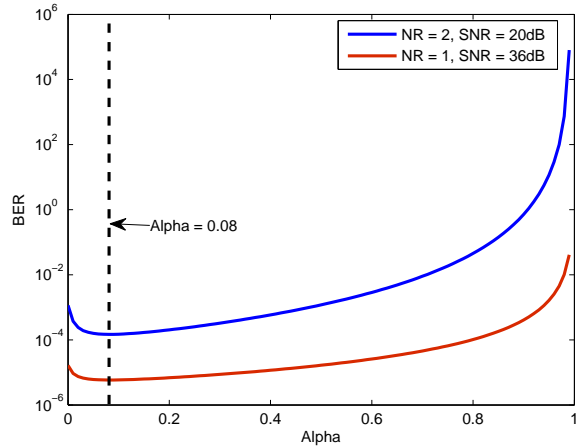


Fig. 8. ABEP as a function of α .

5. Conclusion

In this paper, we have proposed an APSK DSM scheme that is able to achieve a full diversity order of $2N_R$, referred to as DFD-SM using APSK. Next we extended the PAC from [15] to the proposed APSK scheme. The presented framework for the PAC can now be applied to any differential scheme utilizing an APSK constellation. A theoretical upper bound on the BER was derived to validate the simulation results of the proposed schemes. It was shown that the proposed DFD-SM using APSK scheme outperforms CDFD-SM [6], and that the proposed PAC applied to DFD-SM using APSK closes the gap in error performance between differential and coherent detection, while exhibiting superior performance over CDFD-SM.

Acknowledgments

The financial assistance of the National Research Foundation (NRF) towards this research is hereby acknowledged.

Opinions expressed and conclusions arrived at, are those of the author and are not necessarily to be attributed to the NRF. The authors would like to thank K. Kadathlal for his assistance.

References

- [1] MESLEH, R., HAAS, H., SINANOVIC S., et al. Spatial modulation. *IEEE Transactions on Vehicular Technology*, 2008, vol. 57, no. 4, p. 2228–2242. DOI: 10.1109/TVT.2007.912136
- [2] BIAN, Y., WEN, M., CHENG, X. et al. A differential scheme for spatial modulation. In *Proceedings of the 2013 IEEE Global Communications Conference (GLOBECOM)*. 2013, p. 3925–3930. DOI: 10.1109/GLOCOM.2013.6831686
- [3] BIAN, Y., CHENG, X., WEN, M., et al. Differential spatial modulation. *IEEE Transactions on Vehicular Technology*, 2015 vol. 64, no. 7, p. 3262–3268. DOI: 10.1109/TVT.2014.2348791
- [4] WEN, M., DING, Z., CHENG, X., et al. Performance analysis of differential spatial modulation with two transmit antennas. *IEEE Communications Letters*, 2014, vol. 18, no. 3, p. 475–478. DOI: 10.1109/LCOMM.2014.012014.132524
- [5] ISHIKAWA, N., SUGIURA, S. Unified differential spatial modulation. *IEEE Wireless Communications Letters*, 2014, vol. 3, no. 4, p. 337–340. DOI: 10.1109/LWC.2014.2315635
- [6] ZANG, W., YIN, Q., DENG, H. Differential full diversity spatial modulation and its performance analysis with two transmit antennas. *IEEE Wireless Communications Letters*, 2015, vol. 19, no. 4, p. 677–680. DOI: 10.1109/LCOMM.2015.2403859
- [7] RAJASHEKAR, R., ISHIKAWA, N., SUGIURA, S., et al. Full-diversity dispersion matrices from algebraic field extensions for differential spatial modulation. *IEEE Transactions on Vehicular Technology*, 2017, vol. 66, no. 1, p. 385–394. DOI: 10.1109/TVT.2016.2536802
- [8] CHOW, Y. C., NIX, A. R., MCGEEHAN, J. P. Analysis of 16-APSK modulation in AWGN and Rayleigh fading channel. *Electronic Letter*, 1992, vol. 28, no. 17, p. 1608–1610. DOI: 10.1049/el:19921023
- [9] XIA, X. Differentially en/decoded orthogonal space-time block codes with APSK signals. *IEEE Communications Letters*, 2002, vol. 6, no. 4, p. 150–152. DOI: 10.1109/4234.996040
- [10] MARTIN, P. A. Differential spatial modulation for APSK in time-varying fading channels. *IEEE Communications Letters*, 2015, vol. 19, no. 7, p. 1261–1264. DOI: 10.1109/LCOMM.2015.2426172
- [11] LIU, J., DAN, L., YANG, P., et al. High-rate APSK-aided differential spatial modulation: design method and performance analysis. *IEEE Communications Letters*, 2017, vol. 21, no. 1, p. 168–171. DOI: 10.1109/LCOMM.2016.2610962
- [12] LI, L., FANG, Z., ZHU, Y., et al. Generalized differential transmission for STBC systems. In *Proceedings of the 2008 IEEE Global Communications Conference (GLOBECOM)*. 2008, p. 1–5. DOI: 10.1109/GLOCOM.2008.ECP.836
- [13] FANG, Z., LI, L., BAO, X., et al. Generalized differential modulation for amplify-and-forward wireless relay networks. *IEEE Transactions on Vehicular Technology*, 2009, vol. 58, no. 6, p. 3058–3062. DOI: 10.1109/TVT.2008.2012125
- [14] FANG, Z., LIANG, F., LI, L., et al. Performance analysis and power allocation for two-way amplify-and-forward relaying with generalized differential modulation. *IEEE Transactions on Vehicular Technology*, 2014, vol. 63, no. 2, p. 937–942. DOI: 10.1109/TVT.2013.2279856

- [15] DWARIKA, K., XU, H. Power allocation and low complexity detector for differential full diversity spatial modulation using two transmit antennas. *Radioengineering*, 2017, vol. 26, no. 2, p. 461–469. DOI: 10.13164/re.2017.0461
- [16] BEKO, M., XAVIER, J., BARROSO, V. Noncoherent communication in multiple-antenna systems: receiver design and codebook construction. *IEEE Transactions on Signal Processing*, 2007, vol. 55, no. 12, p. 5703–5715. DOI: 10.1109/TSP.2007.901151
- [17] BEKO, M., XAVIER, J., BARROSO, V. Further results on the capacity and error probability analysis of noncoherent MIMO systems in the low SNR regime. *IEEE Transactions on Signal Processing*, 2008, vol. 56, no. 7, p. 2915–2930. DOI: 10.1109/TSP.2008.917363

About the Authors ...

Kavishaur DWARIKA received his B.Sc. and M.Sc. degree in Electronic Engineering from the University of KwaZulu-Natal, South Africa, in 2014 and 2016, respectively. His research interests include wireless communications and digital signal processing.

Hongjun XU (MIEEE, 07) received the B.Sc. degree from the University of Guilin Technology, Guilin, China, in 1984; the M.Sc. degree from the Institute of Telecontrol and Telemeasure, Shi Jian Zhuang, China, in 1989; and the Ph.D. degree from the Beijing University of Aeronautics and Astronautics, Beijing, China, in 1995. From 1997 to 2000, he was a Postdoctoral Fellow with the University of Natal, Durban, South Africa, and Inha University, Incheon, Korea. He is currently a Professor with the School of Engineering at the University of KwaZulu-Natal, Durban. He is the author of more than 25 journal papers. His research interests include wireless communications and digital systems.

Appendix 1

Using the PEP method [6], [11], [16], [17], following (19), the PEP for the PAC applied to DFD-SM using APSK is given by

$$P(\mathbf{X}_{\text{norm}}^{(t)} \rightarrow \hat{\mathbf{X}}_{\text{norm}}^{(t)}) = P\left(\left\|\mathbf{Y}_{\text{norm}}^{(t)} - r_p^{(t)} \mathbf{Y}_{\text{ref}} \mathbf{S}^{(t)}\right\|_F^2 - \left\|\mathbf{Y}_{\text{norm}}^{(t)} - \hat{r}_p^{(t)} \mathbf{Y}_{\text{ref}} \hat{\mathbf{S}}^{(t)}\right\|_F^2 > 0\right). \quad (23)$$

Substituting $\mathbf{Y}_{\text{ref}} = \mathbf{H}_{\text{ref}} \mathbf{X}_{\text{ref}} + \mathbf{N}_{\text{ref}}$ and $\mathbf{Y}_{\text{norm}}^{(t)} = \mathbf{H}_{\text{norm}}^{(t)} \mathbf{X}_{\text{norm}}^{(t)} + \mathbf{N}_{\text{norm}}^{(t)}$, where $\mathbf{H}_{\text{ref}} = \mathbf{H}_{\text{norm}}^{(t)} = \mathbf{H}$ we can simplify (23) into

$$P(\mathbf{X}_{\text{norm}}^{(t)} \rightarrow \hat{\mathbf{X}}_{\text{norm}}^{(t)}) = P\left(\|\mathbf{W}_1\|_F^2 > \left\|\mathbf{H}(\mathbf{X}_{\text{norm}}^{(t)} - \hat{\mathbf{X}}_{\text{norm}}^{(t)}) + \mathbf{W}_2\right\|_F^2\right) \quad (24)$$

where $\mathbf{W}_1 = \mathbf{N}_{\text{norm}}^{(t)} - r_p^{(t)} \mathbf{N}_{\text{ref}} \mathbf{S}^{(t)}$ and $\mathbf{W}_2 = \mathbf{N}_{\text{norm}}^{(t)} - \hat{r}_p^{(t)} \mathbf{N}_{\text{ref}} \hat{\mathbf{S}}^{(t)}$. Proceeding with the analysis we have

$$P(\mathbf{X}_{\text{norm}}^{(t)} \rightarrow \hat{\mathbf{X}}_{\text{norm}}^{(t)}) = P(\zeta > \|\mathbf{D}\|_F^2) \quad (25)$$

where $\zeta = \text{Tr}(\mathbf{W}_2^H \mathbf{D} + \mathbf{D}^H \mathbf{W}_2)$ [11]. For any given channel realization, it can now be seen that ζ is a complex-valued Gaussian random variable with zero mean and variance of

$$\sigma_\zeta^2 = 2\left(\sigma_{\text{norm}}^2 + \sigma_{\text{ref}}^2 |\hat{r}_p^{(t)}|^2\right) \|\mathbf{D}\|_F^2. \quad (26)$$

For $\mathbf{X}_{\text{ref}} = \mathbf{I}_2$, the average value of $|\hat{r}_p^{(t)}|^2$ is 1 [9] and thus follows a $CN(0, 2\sigma_{\text{eff}}^2 \|\mathbf{D}\|_F^2)$ distribution. Hence the PEP can be determined as

$$P(\mathbf{X}_{\text{norm}}^{(t)} \rightarrow \hat{\mathbf{X}}_{\text{norm}}^{(t)}) = E_{\mathbf{H}} \left[Q \left(\sqrt{\frac{\|\mathbf{H}(\mathbf{X}_{\text{norm}}^{(t)} - \hat{\mathbf{X}}_{\text{norm}}^{(t)})\|_F^2}{2\sigma_{\text{eff}}^2}} \right) \right]. \quad (27)$$

Following the remaining steps of the derivation, we end up with the final result of

$$P(\mathbf{X}_{\text{norm}}^{(t)} \rightarrow \hat{\mathbf{X}}_{\text{norm}}^{(t)}) \leq \frac{\sigma_{\text{eff}}^{(2\kappa N_R)} 4^{(\kappa N_R)} (2\kappa N_R - 1)!!}{2 \left(\|\mathbf{Y}_{v_i}\|_F^2 \cdots \|\mathbf{Y}_{v_k}\|_F^2\right)^{N_R} (2\kappa N_R)!!} = \frac{(\sigma_{\text{eff}}^2/2)^{(\kappa N_R)} 8^{(\kappa N_R)} (2\kappa N_R - 1)!!}{2 \left(\|\mathbf{Y}_{v_i}\|_F^2 \cdots \|\mathbf{Y}_{v_k}\|_F^2\right)^{N_R} (2\kappa N_R)!!}. \quad (28)$$